EFFECT OF TURBULENCE CHARACTERISTICS ON LOCAL FLAME STRUCTURE OF H_2-AIR PREMIXED FLAMES

Yuzuru Nada, Mamoru Tanahashi, Toshio Miyauchi
Department of Mechanical and Aerospace Engineering,
Tokyo Institute of Technology
Ookayama, Meguro-ku, Tokyo 152-8552, Japan
ynada@mes.titech.ac.jp, mtanahas@mes.titech.ac.jp, tmiyauch@mes.titech.ac.jp

ABSTRACT

Direct numerical simulations (DNS) of turbulent premixed flames are conducted to investigate effects of turbulence characteristics on the local flame structure. Detailed kinetic mechanism including 12 reactive species and 27 elementary reactions is used to represent hydrogen-air reaction in turbulence. Numerical conditions of DNSs can be classified into wrinkled flamelets regime, corrugated flamelets regime and thin reaction zones near the boundary of Karlovitz number $Ka = 1.0$ of turbulent combustion diagram. For all cases, the distribution of heat release rate shows three-dimensionally connected sheet-like feature, even though the heat release rate is highly fluctuating along the flame front. The heat release rate tends to increase at the flame fronts convex toward the burned side. For the turbulent premixed flames in corrugated flamelets regime, the handgrip structure is produced by the intrusion of the coherent fine scale eddy into the flame and the heat release rate in this structure increases up to 1.2 times of that of laminar flame. The mechanism of heat release rate increase in this structure is clarified by discussing the balance of elementary reactions. In the wrinkled flamelets regime, the spire-like structure of the flame front can be observed. These structure are created by the coherent fine scale eddies of turbulence. By identifying flame elements in turbulence, their statistical characteristics are also discussed.

INTRODUCTION

The local flame structure in turbulence has been considered to depend on the ratios of turbulence intensity to laminar burning velocity (u'/S_L) and integral length scale to laminar flame thickness (l/δ_F) (Peters, 2000). From these ratios, the local flame structure has been classified into wrinkled flamelets regime, corrugated flamelets regime, thin reaction zones and broken reaction zones. In direct numerical simulation (DNS), systematic selection of u'/S_L and l/δ_F is relatively easy compared with the experiments, and all of the information concerning the flame structure can be obtained. Baum et al. (1994a) have conducted two-dimensional DNSs of hydrogen-air turbulent premixed flames with detailed kinetics mechanism and have shown effects of turbulence characteristics on local flame structure. Tanahashi et al. (2001) have clarified effects of turbulence intensity on the local flame structure from two-dimensional DNSs of hydrogen-air turbulent premixed flames. They showed that isolated pockets of unburned gas are observed in the burned side.

Due to remarkable developments of computer technology, details of fine scale motions in turbulence have been investigated by DNS. Tanahashi et al. (1997) have shown that homogeneous isotropic turbulence consists of a lot of similar tube-like eddies which accompany strong swirling motions. These tube-like eddies are called as 'coherent fine scale eddies'. Coherent fine scale eddies are universal structure of turbulence, and mean diameter of these eddies is about 8 times of Kolmogorov micro scale (η) and maximum of the mean azimuth velocity is about 0.6 times of the root mean square of velocity fluctuation (u'_{rms}) in low Reynolds number cases. Recently, it has been reported that the maximum azimuthal velocity can be scaled by the Kolmogorov velocity, whereas the strong coherent fine scale eddies possess azimuthal velocity of the order of u'_{rms} (Miyauchi et al., 2002).

The coherent fine scale eddies may influence the local flame structure of turbulent flames because of their strong swirling motion. Tanahashi et al. (1999a, 2000) have conducted three-dimensional DNSs of hydrogen-air turbulent premixed flames to investigate the interaction between flame and coherent fine scale eddies, and clarified that the local flame structure depends on the angle between flame surface and axis of coherent fine scale eddy. Bell et al. (2002) have conducted three-dimensional DNSs of lean methane-air turbulent premixed flames using low Mach number approximation and reduced kinetic mechanism. They have investigated effects of turbulence/flame interaction on the flame chemistry. Tanahashi et al. (1999a, 2000, 2002) have also clarified the local flame structure in corrugated flamelets regime and thin reaction zones. Although it has been believed that the local flame structure in wrinkled flamelets regime can be approximated by that of laminar flame, the precise structure has not been clarified yet. In this study, effects of turbulence characteristics on the local flame structure are investigated by three-dimensional DNSs of hydrogen-air turbulent premixed flames.

DNS OF HYDROGEN-AIR TURBULENT PREMIXED FLAMES

Details of the governing equations can be found in Miyauchi et al. (1996). A detailed kinetic mechanism (Gutheil et al., 1993) which includes 27 elementary reactions and 12 reactive species (H_2, O_2, H_2O, O, H, OH, HO_2, H_2O_2, N_2, N, NO_2 and NO) is used to represent hydrogen-air reaction in turbulence. The temperature dependence of the viscosity, the thermal conductivity and the diffusion coefficients are taken into account by linking CHEMKIN packages (Kee et al., 1986; 1989) with modifications for vector/parallel computations. Figure 1 shows a schematic of

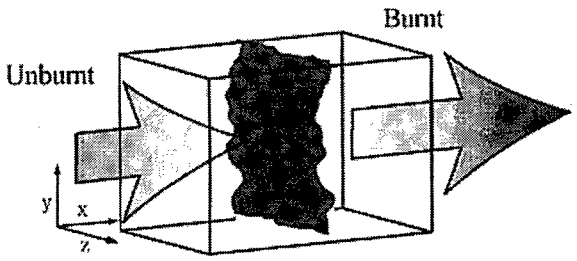

Figure 1: Geometry of the flow field.

Table 1: Numerical parameters for DNS of hydrogen-air turbulent premixed flames.

	Re_λ	l/δ_F	u'/S_L	D/δ_L	l/δ_L
Case 1	37.4	168.6	0.85	0.78	3.38
Case 2	37.4	84.3	1.70	0.39	1.69
Case 3	37.4	42.2	3.41	0.19	0.85

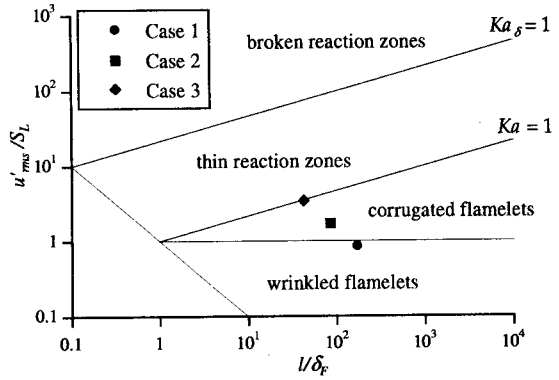

Figure 2: Turbulent combustion diagram.

the flow field used in this study. The governing equations are discretized by 4th-order central difference scheme in the x direction and by a Fourier spectral method in the y and z directions. The boundary conditions in the x direction are NSCBC (Poinsot and Lele, 1992; Baum et al., 1994b) and those in the y and z directions are periodic. Time integration is implemented by the third-order Runge-Kutta scheme.

Numerical parameters of DNSs are listed in Table 1. DNSs are conducted for three cases that have different u'/S_L and l/δ_F. Note that δ_F is defined by $\delta_F = \nu/S_L$, where ν denotes kinematic viscosity of the unburned mixture (Peters, 2000). In the present study, DNS of Case 1 is conducted. Case 2 and Case 3 were conducted by Tanahashi et al. (1999a, 2000, 2002). A hydrogen-air mixture in the unburned side is set to $\phi = 1.0$ at 0.1MPa and 700K. The inflow boundary condition for the velocity field is given as $u_{in}(y,z,t) = S_L + u'(y,z,t)$. The turbulence $u'(y,z,t)$ was obtained by the preliminary DNS of homogeneous isotropic turbulence by a spectral method and the Reynolds number based on Taylor micro scale Re_λ is 37.4. In our previous study (Tanahashi et al., 1999a), it has been shown that the coherent fine scale eddy in turbulence plays important roles on the local flame structure of the turbulent premixed flames. In Table 1, the ratios of the most expected diameter $D(=8\eta)$ of the coherent fine scale eddy to the laminar flame thickness δ_L are presented. δ_L is defined by $\delta_L = (T_b - T_u)/(\partial T/\partial x)\mathrm{max}$, where T_u and T_b denote temperature in the unburned and burned side, respectively. In Case 1, this diameter is about $0.8\delta_L$.

In Fig. 2, locations of each DNS are plotted on the turbulent combustion diagram proposed by Peters (2000). Case 1, Case 2 and Case 3 are classified in wrinkled flamelets regime, corrugated flamelets regime and thin reaction zones near the boundary of Karlovitz number $Ka = 1.0$, respectively.

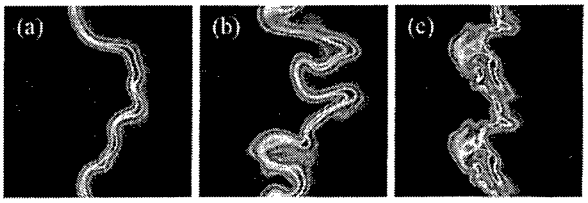

Figure 3: Distributions of the heat release rate on a typical x-z plane for Case 1(a), Case 2(b) and Case 3(c).

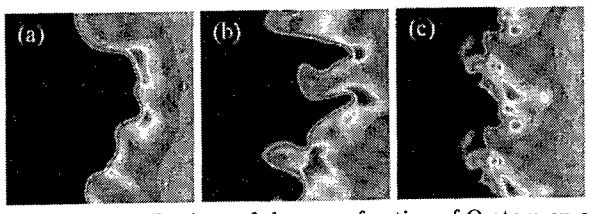

Figure 4: Distributions of the mass fraction of O atom on a typical x-z plane for Case 1(a), Case 2(b) and Case 3(c).

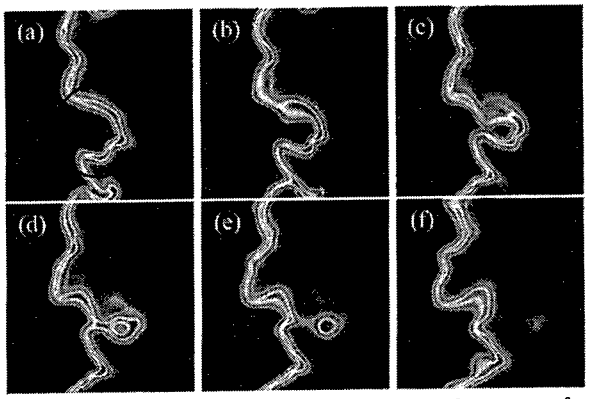

Figure 5: Successive distributions of heat release rate for Case 2 with time interval of $0.2\tau_l$.

LOCAL FLAME STRUCTURE OF TURBULENT PREMIXED FLAMES

Three-dimensional Feature of Turbulent Premixed Flames

The distributions of heat release rate on a typical x-z plane for all cases are shown in Fig. 3. The size of visualized region in Fig. 3 is 5mm × 5mm. In Case 1, distribution of heat release rate shows sheet-like feature. Along the flame front, the heat release rate is fluctuating owing to turbulence motion. The fluctuations of heat release rate in corrugated flamelets regime and thin reaction zones are larger than that in wrinkled flamelets regime as shown in Fig. 3(b) and (c). Even though the heat release rate is highly fluctuating, its distribution shows three-dimensionally connected sheet-like feature for all cases (Tanahashi et al., 2002). The flame convex toward burned side shows high heat release rate compared with that of laminar flame in Case 1. Our previous studies (Tanahashi et al., 1999a; 2000; 2002) have clarified that distributions of heat release rate in corrugated flamelets regime and thin reaction zones show the same tendency.

Miyauchi et al. (1997) have investigated the mechanism of the increase of heat release rate in two-dimensional hydrogen-air turbulent premixed flames, and clarified the distinct relation between O atom and heat release rate. Figure 4 shows the distributions of mass fraction of O atom on a typical x-z plane. The mass fraction of O atom tends to increase behind the flame with high heat release rate for all

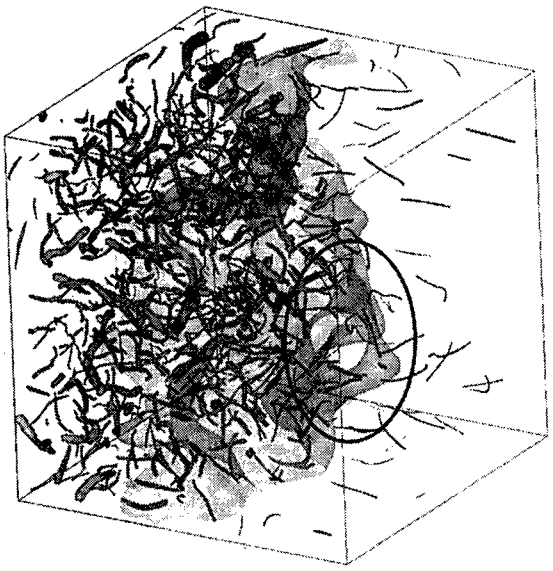

Figure 6: Contour surface of temperature and the axes of coherent fine scale eddies.

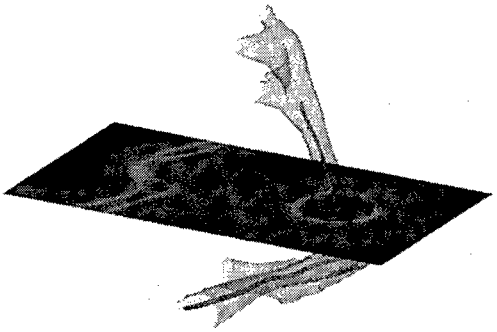

Figure 7: Contour surface of heat release rate and the axes of coherent fine scale eddies.

cases. These results suggest that the increase of heat release rate is attributed to the same mechanism as that shown by Miyauchi et al. (1997).

The successive distributions of heat release rate on a different plane are shown in Fig. 5 for Case 2 with time interval of $0.2\tau_l$, where τ_l denotes eddy turnover time ($= l/u'$). The largely wrinkled flame toward the burned side appears as shown by the circle in Fig. 5(a). At the cusp of the flame, the maximum heat release rate is about 1.1 times of that of laminar flame (ΔH_L). This cusp of the flame moves toward the burned side and then the unburned mixture appears behind flame front. This unburned mixture seems to be isolated in the burned gas from the cross sectional viewpoint in Fig. 5(e). The maximum heat release rate in the unburned mixture reaches to about $1.2\Delta H_L$ and decreases rapidly down to $0.3\Delta H_L$ as shown in Fig. 5(f). In the previous study by Chen et al. (1998), similar results have been reported from two-dimensional DNS of methane-air turbulent premixed flames and the presence of unburned mixture like a pocket has shown even in low intensity turbulence. However, three-dimensional structure of unburned mixture is not clarified. To investigate this issue, axes of coherent fine scale eddies are determined by the eddy identification scheme by Tanahashi et al. (1999b).

Figure 6 shows the contour surface of temperature and axis distribution of coherent fine scale eddies at the same time as in Fig. 5(e). The contour level of temperature is 1400K. To show the axes of coherent fine scale eddies in the

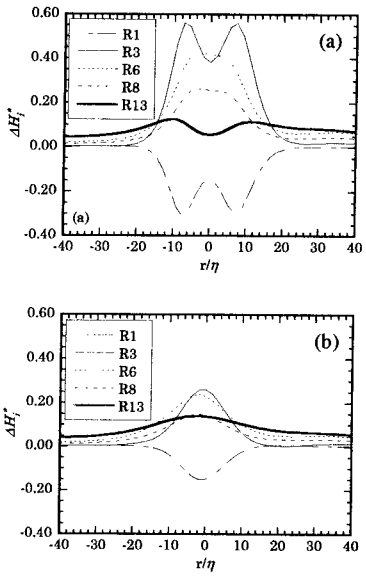

Figure 8: Contributions of elementary reactions on heat release rate in the handgrip structure at different times.

unburned mixture, the half-transparent contour surfaces are used. The diameter of the axis in this figure is drawn to be proportional to square root of second invariant of velocity gradient tensor ($Q = (W_{ij}W_{ij} - S_{ij}S_{ij})/2$), where $S_{ij} = (\partial u_i/\partial x_j + \partial u_j/\partial x_i)/2$ and $W_{ij} = (\partial u_i/\partial x_j - \partial u_j/\partial x_i)/2$ are symmetric and asymmetric parts of velocity gradient tensor, respectively. As shown by the circle in Fig. 6, the unburned mixture shows the three-dimensional structure like a handgrip and is connected three-dimensionally with the unburned side. The several coherent fine scale eddies appear in the handgrip structure. Most of coherent fine scale eddies in the burned side tend to decay rapidly by the increase of viscosity. The axis of coherent fine scale eddy in the burned side tends to be parallel to the direction of mean flame propagation by the effect of expansion. On the contrary, the axes in the handgrip structure are nearly perpendicular to the direction of mean flame propagation. The strong perpendicular coherent fine scale eddy intrudes into the flame and transports the unburned mixture, which leads to the formation of the handgrip structure. Figure 7 shows the contour surface of heat release rate and axes of coherent fine scale eddies near the handgrip structure. The contour level of heat release rate is $1.1\Delta H_L$. Distribution of heat release rate on the same plane as in Fig. 5(e) is also shown. The region with high heat release rate is generated around coherent fine scale eddies. Since the unburned mixture transported with the eddy burns out rapidly, the heat release rate increases around the eddy.

The contributions of elementary reactions on heat release rate are shown on a line across the center of unburned mixture at two different times in Fig. 8. In these figures, abscissa is normalized by the Kolmogorov micro scale of unburned turbulence and the heat release rate of each elementary reaction is normalized by ΔH_L. Hereafter, * denotes normalization by δ_L, S_L and ΔH_L. Figure 8(a) corresponds to the time in Fig. 5(e) and Fig. 8(b) represents the results after $0.1\tau_l$. Miyauchi et al. (1997) have investigated the contributions of elementary reactions at the flame front and clarified main elementary reactions for heat release rate as follows;

R1 : $H + O_2 \Leftrightarrow OH + O$,

R3 : $H_2 + OH \Leftrightarrow H_2O + H$,

R6 : $H + O_2 + M \Leftrightarrow HO_2 + M$,

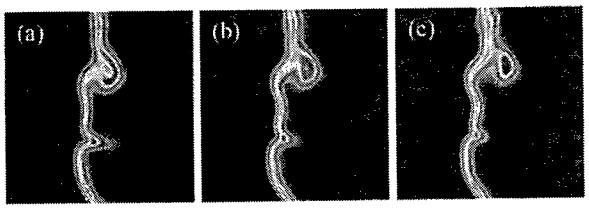

Figure 9: Successive distributions of heat release rate for Case 1 with time interval of $0.04\tau_l$.

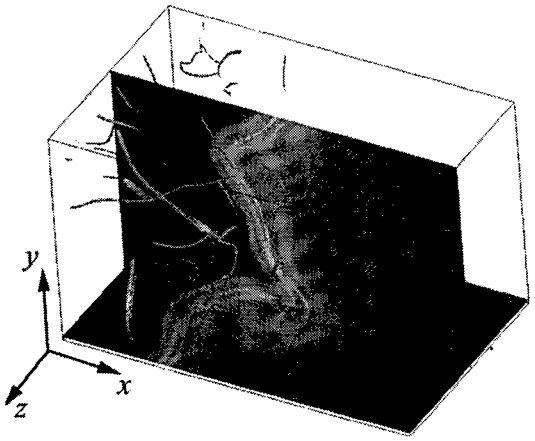

Figure 10: Distributions of heat release rate and the axes of coherent fine scale eddies for Case 1.

R8 : $H + HO_2 \Leftrightarrow OH + OH$.

In Fig. 8(a), the elementary reaction R6, which is enhanced in the preheat zones, shows high contribution in the whole region of the handgrip structure. The flame front is generated around the unburned mixture and the temperature of unburned mixture increases up to 1100K, which indicates that unburned mixture in the handgrip structure is in the similar condition as in the preheat zones. Therefore, the contribution of R6 in the whole region of the handgrip structure increases. Even though the reaction rate of each elementary reaction is higher than that of laminar flame, main elementary reactions do not change. After $0.1\tau_l$, main reactions show low reaction rate owing to the decrease of mole fractions of H_2 and O_2. Intermediate species such as H, O and OH are produced through the main reactions, which leads to the increase of R13 reaction rate.

R13 : $H + OH + M \Leftrightarrow H_2O + M$.

These results imply that the increase of heat release rate in the handgrip structure is attributed to the same mechanism as in the flame front of a laminar case except for final stage in which the enhancements of elementary reactions are mainly related with intermediate species.

Figure 9 shows successive distributions of heat release rate for Case 1 at three different times on a typical x-z plane. The time interval is $0.04\tau_l$. Although the turbulent premixed flame of Case 1 is classified in wrinkled flamelets regime, the unburned mixture with high heat release rate is formed behind flame front. The distributions of heat release rate on the x-y and x-z planes with axes of coherent fine scale eddies are shown in Fig. 10. The visualized x-z plane is same as that in Fig. 9. The distribution on the x-y plane shows that the unburned mixture possesses spire-like structure. Since the perpendicular eddy at the cusp of spire structure can be observed, the spire structure is considered to be produced by the intrusion of the coherent fine scale eddy. Three-dimensional structures like handgrip or spire enhance the local heat release rate and lead to the increase of turbulence burning velocity.

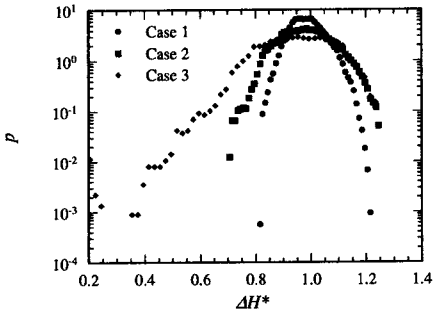

Figure 11: Probability density functions of the local heat release rate.

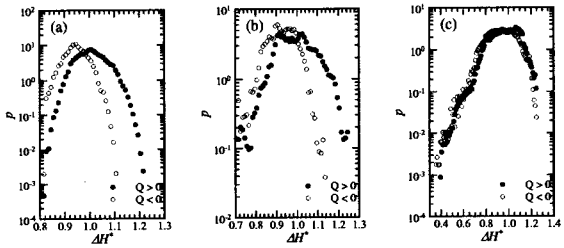

Figure 12: Probability density functions of the local heat release rate conditioned with the sign of second invariant of velocity gradient tensor.

Statistical Characteristics of Local Flame Structure

To clarify effects of turbulence characteristics on local flame structure, the statistical characteristics of flame elements are investigated. The flame fronts are defined as points with the local maximum temperature gradient. Probability density functions (pdf) of local heat release rate are shown in Fig. 11 for all cases. The local heat release rate is the maximum heat release rate in the flame element and normalized by ΔH_L. In Case 1, which is classified into wrinkled flamelets regime, the pdf of heat release rate shows a sharp peak at $1.0\Delta H_L$ and the fluctuation of heat release rate is about $0.2\Delta H_L$. With the increase of turbulence intensity and decrease of turbulence characteristic length, the fluctuation of heat release rate becomes large. In Case 3, the pdf is nearly flat in the range of $0.9\Delta H_L$ to $1.1\Delta H_L$ and the maximum heat release rate reaches to $1.3\Delta H_L$ and the minimum also decreases to less than half of ΔH_L.

The pdf of heat release rate is conditioned with the sign of Q at the flame front to investigate the effect of coherent fine scale eddies on the local heat release rate. From the definition, the rotation rate ($W_{ij}W_{ij}$) exceeds the strain rate ($S_{ij}S_{ij}$) in the region with $Q > 0$. These regions represent coherent fine scale eddies of turbulence approximately. In the regions with $Q < 0$, the coherent fine scale eddy does not exist, and strain field dominates the flow. In these regions, the dissipation rate of turbulent kinetic energy is high. Figure 12 shows the conditional pdfs of the heat release rate. In all cases, probability of flame element with high heat release rate for $Q > 0$ is higher than that for $Q < 0$, which means that rotation dominant regions tend to enhance the heat release rate and strain dominant regions tend to suppress it. In Case 2, which is classified into corrugated flamelets regime, Tanahashi et al. (1999a) have clarified that the coherent fine scale eddy parallel to flame front transports unburned gas into the flame front by strong swirling motion and generates the region with high heat release rate. These results indicate that coherent fine scale eddy tends to enhance the heat release rate for all cases.

Figure 13 shows the pdfs of flame thickness of local

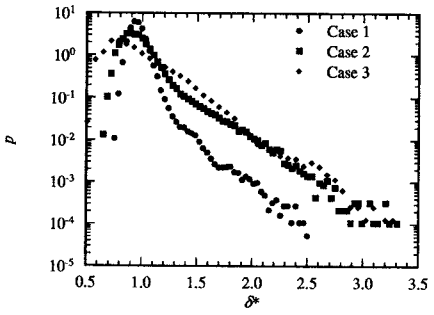

Figure 13: Probability density functions of the local flame thickness.

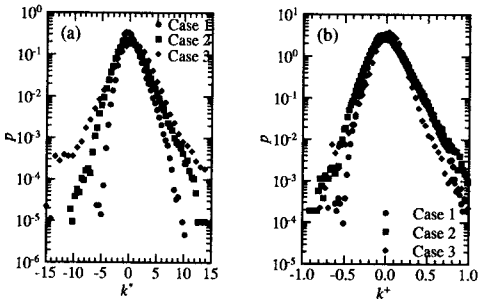

Figure 14: Probability density functions of curvature of flame front.

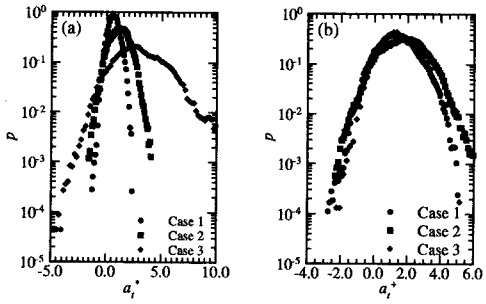

Figure 15: Probability density functions of tangential strain rate.

flame elements. The local flame thickness is defined by $\delta = (T_b - T_u)/(\boldsymbol{n} \cdot \mathrm{grad}T)_{\max}$, where $\boldsymbol{n}$ is an unit vector normal to the temperature gradient. The local flame thickness is normalized by δ_L. The pdf of Case 1 shows the peak near $1.0\delta_L$. In Case 3, most expected flame thickness becomes thin and decreases to $0.8\delta_L$. For all cases, the fluctuation of flame thickness is large. Even in Case 1, the maximum and minimum thickness are $2.5\delta_L$ and $0.8\delta_L$. The fluctuation in Case 3 is larger than other cases and flame elements with $0.5\delta_L$ to $3.3\delta_L$ can be observed.

The curvature of flame front and strain rate on the flame surface are important parameters to characterize local flame structure. The pdfs of the curvature of flame front are shown in Fig. 14. The curvature is defined as $k = 1/r_1 + 1/r_2$, where r_1 and r_2 denote two curvature radii of the flame surface. The flame element convex toward the burned side has positive value and the curvature is normalized by δ_L in Fig. 14(a) and by η in Fig. 14(b). In Case 3, probability of flame element with large curvature increases compared with other cases as shown in Fig. 14(a). However, if curvature is normalized by η, the pdfs show a good agreement and the minimum radius of flame front is about 1.0η. These results

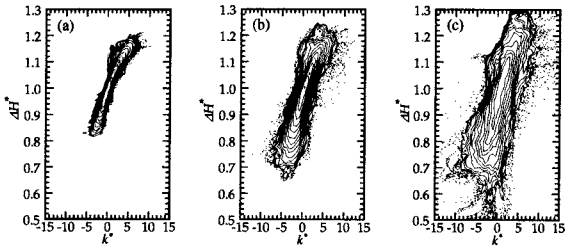

Figure 16: Joint probability density functions of the curvature and the local heat release rate for Case 1(a), Case 2(b) and Case 3(c).

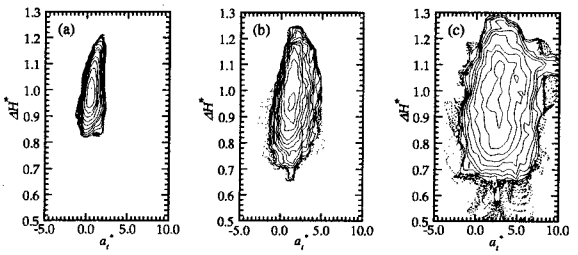

Figure 17: Joint probability density functions of the tangential strain rate and the local heat release rate for Case 1(a), Case 2(b) and Case 3(c).

show that the curvature of flame front depends on turbulence characteristic length in the unburned side.

Figure 15 shows the pdfs of the strain rate tangential to flame surface. The tangential strain rate at the flame front is defined as $a_t = \boldsymbol{t}_1 \boldsymbol{t}_1 : \nabla \boldsymbol{u} + \boldsymbol{t}_2 \boldsymbol{t}_2 : \nabla \boldsymbol{u}$, where $\boldsymbol{t}_1$ and $\boldsymbol{t}_2$ represent unit vectors tangential to the flame front and are satisfying a relation of $\boldsymbol{t}_1 \cdot \boldsymbol{t}_2 = 0$ (Candel and Poinsot, 1990). The positive tangential strain represents stretch and the negative strain does compression. The tangential strain rate is normalized by S_L and δ_L in Fig. 15(a) and by u' and λ in Fig. 15(b). In Fig. 15(a), pdfs of tangential strain rate show the peak at positive value for all cases, which means that most of flame element are stretched by the turbulence motion. The maximum and most expected tangential strain rate of Case 3 are larger than those of other cases. If the tangential strain rate is normalized by turbulence characteristics as shown in Fig. 15(b), pdfs of the tangential strain rate for all cases coincide very well, and the peak value is observed at the inverse of Taylor time scale. From these results, it is considered that the tangential strain rate at the flame fronts can be scaled by the turbulence characteristics in the unburned gas.

Figure 16 shows the joint pdfs of the curvature of flame front and the local heat release rate. The curvature of flame front is normalized by δ_L. For all cases, the local heat release rate shows strong correlation with the curvature and increases with the increase of the curvature. Furthermore, the gradient of ΔH^* with respect to k^* is nearly identical for all cases. Figure 17 shows joint pdfs of the tangential strain rate and local heat release rate. Tangential strain rate is normalized by S_L and δ_L. In Case 1, local heat release rate shows a correlation with the tangential strain rate and shows larger value in the stretched flame elements. However, in Case 3, the distinct correlation can not be observed.

CONCLUSION

In this study, direct numerical simulations of hydrogen-air premixed flames propagating in homogeneous isotropic turbulence are conducted to investigate effects of turbulence characteristics on the local flame structure, and the following

conclusions are obtained.

(1) For all cases, the distributions of heat release rate show three-dimensionally connected sheet-like feature, even though the heat release rate is highly fluctuating along the flame front.

(2) For the turbulent premixed flames in corrugated flamelets regime, the handgrip structure is produced by intrusion of the coherent fine scale eddy into the flame. The heat release rate in this structure increases, which is attributed to the same mechanism as in flame front of a laminar case. In the wrinkled flamelets regime, the spire-like structure of the flame front is created due to the coherent fine scale eddies of turbulence.

(3) Flame elements in thin reaction zones show large fluctuation of heat release rate compared with those in flamelets regime. The coherent fine scale eddies tend to enhance the heat release rate and strain dominant regions tend to suppress it. Most expected flame thickness in thin reaction zones is thinner than those in flamelets regime. The curvature and tangential strain rate of the flame fronts can be scaled by the turbulence characteristics of unburned gas. For all cases, the curvature shows the strong correlation with local heat release rate and flame elements convex toward the burned gas tend to show high heat release rate.

ACKNOWLEDGMENTS

This work is partially supported by Grant-in-Aid for Scientific Research (A) of Japan Society for the Promotion of Science and by the collaborative research project on "Smart Control of Turbulence: A Millennium Challenge for Innovative Thermal and Fluids Systems" of the Ministry of Education, Culture, Sports, Science and Technology.

REFERENCES

Baum, M., Poinsot, T., Hawaorth, D. and Darabiha, N., 1994a, "Direct Numerical Simulation of $H_2/O_2/N_2$ Flames with Complex Chemistry in Two-dimensional Turbulent Flow", *Journal of Fluid Mechanics*, Vol. 281, pp. 1-32.

Baum, M., Poinsot, T. and Thevenin, D., 1994b, "Accurate Boundary Conditions for Multicomponent Reactive Flows", *Journal of Computational Physics*, Vol. 116, pp. 247-261.

Bell, J. B., Day, M. S. and Grcar, J. F., 2002, "Numerical Simulation of Premixed Turbulent Methane Combustion", *Proceedings of the Combustion Institute*, Vol. 29, in press.

Candel, S. M. and Poinsot, T. J., 1990, "Flame Stretch and the Balance Equation for the Flame Area", *Combustion Science and Technology*, Vol. 70, pp. 1-15.

Chen, J. H., Echekki, T. and Kollmann, W., 1998, "The Mechanism of Two-dimensional Pocket Formation in Lean Premixed Methane-Air Flames with Implications to Turbulent Combustion", *Combustion and Flame*, Vol. 116, pp. 15-48.

Gutheil, E., Balakrishnan, G. and Williams, F. A., 1993, "Structure and Extinction of Hydrogen-Air Diffusion Flames", Reduced Kinetic Mechanisms for Applications in Combustion Systems, edited by Peters, N. and Rogg, B., Springer-Verlag, pp. 177-195.

Kee, R. J., Dixon-Lewis, G., Warnatz, J., Coltrin, M. E. and Miller, J. A., 1986, "A Fortran Computer Code Package for the Evaluation of Gas-Phase Multicomponent Transport Properties", Sandia Report, SAND86-8246.

Kee, R. J., Rupley, F. M. and Miller, J. A., 1989, "Chemkin-II: a Fortran Chemical Kinetics Package for the Analysis of Gas Phase Chemical Kinetics", Sandia Report, SAND89-8009B.

Miyauchi, T., Tanahashi, M., Sasaki, K. and Ozeki, T., 1996, "Transport Phenomena in Combustion", Chen, C. H. ed., Taylor and Francis, New York, pp. 1095-1105.

Miyauchi, T., Tanahashi, M., Imamura, Y. and Nada, Y., 1997, "Structure and Fractal Characteristics of H_2-Air Turbulent Premixed Flames", *Proceedings of 1st Asia-Pacific Conference on Combustion*, pp. 278-281.

Miyauchi, T., Tanahashi, M. and Iwase, S., 2002, "Coherent Fine Scale Eddies and Energy Dissipation Rate in Homogeneous Isotropic Turbulence up to $Re_\tau = 220$", *IUTAM Symposium, Reynolds Number Scaling of Turbulent Flow*, in press.

Peters, N., 2000, "Turbulent Combustion", Cambridge University Press.

Poinsot, T. J. and Lele, S. K., 1992, "Boundary Conditions for Direct Simulations of Compressible Viscous Flows", *Journal of Computational Physics*, Vol. 101, pp. 104-129.

Tanahashi, M., Miyauchi, T. and Ikeda, J., 1997, "Scaling Law of Coherent Fine Scale Structure in Homogeneous Isotropic Turbulence", *Proceedings of 11th Symposium on Turbulent Shear Flow*, Vol. 1, pp. 4-17.

Tanahashi, M., Nada, Y., Fujimura, M. and Miyauchi, T., 1999a, "Fine Scale Structure of H_2-Air Turbulent Premixed Flames", *Turbulence and Shear Flow Phenomena - 1*, Eds. Banaerjee, S., and Eaton, J. K., Begell House Inc., pp. 59-64.

Tanahashi, M., Iwase, S., Uddin, MD. A. and Miyauchi, T., 1999b "Three-dimensional Features of Coherent Fine Scale Eddies in Turbulence", *Turbulence and Shear Flow Phenomena - 1*, Eds. Banaerjee, S., and Eaton, J. K., Begell House Inc., pp. 79-84.

Tanahashi, M., Fujimura, M. and Miyauchi, T., 2000, "Coherent Fine-Scale Eddies in Turbulent Premixed Flames", *Proceedings of the Combustion Institute*, Vol. 28, pp. 529-535.

Tanahashi, M., Ito, Y. Yu, Y. and Miyauchi, T., 2001, "The Structure of Hydrogen-Air Premixed Flames in High-Intensity and Small-Scale Turbulence", *Proceedings of 3rd Asia-Pacific Conference on Combustion*, pp. 75-78.

Tanahashi, M., Nada, Y., Ito, Y. and Miyauchi, T., 2002, "Local Flame Structure in the Well-Stirred Reactor Regime", *Proceedings of the Combustion Institute*, Vol. 29, in press.